The multipolar elastic fields of ellipsoidal and polytopal plastic inclusions

Gurrutxaga-Lerma, B.

DOI:
10.1098/rspa.2023.0214

Document Version
Publisher's PDF, also known as Version of record

Citation for published version (Harvard):
Gurrutxaga-Lerma, B 2023, 'The multipolar elastic fields of ellipsoidal and polytopal plastic inclusions', *Proceedings of the Royal Society A: Mathematical, Physical and Engineering Sciences*, vol. 479, no. 2276, 20230214. https://doi.org/10.1098/rspa.2023.0214

PROCEEDINGS A

royalsocietypublishing.org/journal/rspa

Research

Cite this article: Gurrutxaga-Lerma B. 2023 The multipolar elastic fields of ellipsoidal and polytopal plastic inclusions. *Proc. R. Soc. A* **479**: 20230214.
https://doi.org/10.1098/rspa.2023.0214

Received: 28 March 2023
Accepted: 4 August 2023

Subject Areas:
materials science, mechanics

Keywords:
inclusion, multipole, elasticity

Author for correspondence:
B. Gurrutxaga-Lerma
e-mail: b.gurrutxagalerma.1@bham.ac.uk

Electronic supplementary material is available online at https://doi.org/10.6084/m9.figshare.c.6794100.

THE ROYAL SOCIETY PUBLISHING

The multipolar elastic fields of ellipsoidal and polytopal plastic inclusions

B. Gurrutxaga-Lerma

School of Metallurgy and Materials, University of Birmingham, B15 2TT Edgbaston, Birmingham, UK

BG-L, 0000-0002-3626-963X

The article offers a general formulation for the multipolar field expansion of an inclusion. The multipolar moments of arbitrary order for the ellipsoidal inclusion are derived, showing known features of their elastic fields in both the far and near field. Using integer point enumeration theory, the same formulation is extended to all polytopal inclusions, which serve to model faceted inclusions found in, e.g. igneous and metamorphic rocks, particle reinforced composite materials, or as intermetallic precipitates in alloys. A general algorithm for the calculation of the multipolar moments of polytopes of any number of vertices is derived. A number of examples for tetrahedral, cuboidal and dodecahedral inclusions are given. It is shown that the parity of the axial moment function of a polytopal inclusion mirrors the symmetry of the inclusion. This represents the main properties of their elastic fields, including the long- and near-field decay. If the inclusion is symmetric with respect to a given axes, the fields will decay with $1/r^2$ in the far field and $1/r^4$ in the near field. If symmetry along that direction is lost, as is expected in most real inclusions, the decay rate progresses with $1/r^2$ but the near field with $1/r^3$.

1. Introduction

This article concerns the approximation of the elastic fields of a plastic inclusion via their multipolar field expansion. Plastic inclusions serve to model regions in a material that have undergone some form of internal rearrangement, as may be encountered in multicomponent precipitates found in shear zones [1],

multiphase materials [2] including martensites and twins [3,4], or when modelling quantum dots [5,6], to name but a few examples.

The problem of the plastic inclusion was first formulated by Eshelby in 1957, who achieved the explicit solutions to the external elastic fields of an inclusion of ellipsoidal shape in isotropic media [7,8]. Sass *et al.* [9] first studied the elastic fields of a cuboidal inclusion, for which they offered a Fourier series solution; this problem was later reworked by Faivre [10], who achieved the first explicit solution to the elastic fields of a parallelepipedal inclusion in isotropic elasticity. Further geometries have been studied both in the context of homogeneous eigenstrains and isotropic elasticity and for anisotropic materials [11], with different elastic moduli [12], including solutions for the fields of square plate inclusions [13], cuboids [14], cylinders [15], rod-like inclusions [16], concave inclusions [17], toroids [18], generalized formulations for arbitrary closed geometries [19] and polyhedra [6,20].

Even for the simplest cases, such as the original Eshelbian ellipsoidal inclusion, the explicit solutions to the external and internal elastic fields of the inclusion are famously forbidding. The elastic energy and the elastic fields of inclusions of the simplest geometries in isotropic linear elasticity (parallelepipedal [10], ellipsoidal [7,8]) still entail solutions that cannot be expressed in terms of simple functions, and rely on implicit elliptic integrals and on nested hierarchies of such functions and their derivatives. Excluding transversely isotropic materials, for inclusions in anisotropic media only numeric solutions are available [21]. This article is concerned with offering an approximate hierarchy with which to obtain a simple account of the long-range elastic fields of inclusions of ellipsoidal or polytopal shape, whether in an isotropic or anisotropic medium, that can serve to approximate their fields to arbitrary accuracy in the near field as well.

This will be achieved by producing the multipolar expansion of the elastic fields of the inclusion. Multipolar field expansions originate in electrodynamics (cf. [22]) where, taking advantage of the fast decay of the electrodynamic Green's function, they are employed to assimilate complex distributions of charge into localized charge distributions. Similarly to how it is done in electrodynamics, in linear elasticity one can achieve a multipolar field expansion by producing the Taylor series expansion of the elastic field's integral representation formula (q.v. [23]). Each subsequent term in the expansion will be contributed by an induced force dipole, quadrupole, and so on. In both the electromagnetic and elastic cases, the fundamental solution to the field decays with $1/r$, so with increasing multipolar term will be dominated by increasing powers of $1/r$. And because the terms in the expansion are all rational functions, once the multipolar moments are known, the expansion enables a fast estimate of the fields to remarkable accuracy.

In the context of linear elasticity, multipolar field expansions have long been employed to model point defects [24,25], particularly because the trace of the dipolar moment tensor is the relaxation volume of the defect [26], which enables the easy modelling of the dipolar moment tensor if the relaxation volume of the point defect can be calculated from first principles [26,27] or deduced from X-ray diffraction data [28]. Generalized formalisms of the multipolar fields have been offered in the context of reconstruction of seismic sources from estimated low order multipolar moments [29,30], and applied over particular cases to circular voids in plane stress [31], prismatic loops [32], dislocation loops and cracks [33] or to stochastic ensembles of dislocations [34]. They have also been applied to ensembles of dislocations in the context of discrete dislocation dynamics and the fast multipole method [35,36], and in the context of homogenization theory, with the aim of development of effective elastic moduli and constitutive behaviours in composite materials with spherical or ellipsoidal inclusions [37–39].

In §2, this article generalizes prior studies (e.g. [31,39]) of multipolar fields of ellipsoidal inclusions to arbitrary order. Aside from providing an intuitive and computationally cheap means of studying the long and near field of the inclusion, the multipolar expansion of the ellipsoidal inclusion serves as a testing ground for the approach, showcasing how non-obvious known results such as the effect of the inclusion's volume in the far field [40] can be quickly recovered (thereby validating the approach) while facilitating understanding of the near field as

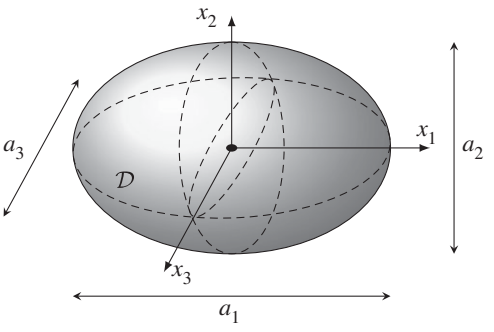

Figure 1. Schematic plot of the ellipsoidal inclusion $\mathcal{D}$.

well. Section 3 extends these efforts to inclusions of convex polytopal geometry of any order, particularly common in materials science, where new phases grow through faceting. This is achieved by exploiting modern developments in integer point enumeration [41], which as will be shown enable the derivation of a general algorithm for the multipolar moments of any order for any convex polytope, be it in two or three dimensions. This approach reveals a number of important features concerning the effect the symmetry of the polytopal inclusion has on its long-range and near-field behaviours, and offers a simple intuitive formula with which to quantify said effects. Section 4 outlines the main findings of the article.

2. Multipolar expansion of an ellipsoidal inclusion

The explicit solution to the elastic fields of an ellipsoidal inclusion was originally given by Eshelby [7,8]. An extension of Eshelby's account to anisotropic elasticity can be found in Mura [23]. Eshelby's inclusion is defined as an ellipsoidal region $\mathcal{D}$ embedded in an infinite, homogeneous, isotropic linear elastic medium $\mathcal{E} \subseteq \mathbb{R}^3$ (figure 1). The region $\mathcal{D}$ is subjected to an unspecific transformation which changes its geometry. This transformation is given by an eigenstrain (or *transformation strain*, or *stress-free strain*) e^*_{ij}, which is defined to be homogeneous for all points $\mathbf{x} \in \mathcal{D}$. As a result of the inclusion $\mathcal{D}$ being constrained by the medium $\mathcal{E}$, mechanical equilibrium considerations at the interface $\partial\mathcal{D}$ between the inclusion and the medium cause a non-trivial elastic field to arise both inside and outside the inclusion.

Owing to the ellipsoidal symmetry of the inclusion, an explicit solution both inside [7] and outside [8] the inclusion can be achieved. A remarkable result is that the inclusion acts as a lacuna (cf. [42–44]), with the strain and stress fields inside the inclusion being homogeneous so long as the inclusion is ellipsoidal [45,46].

(a) General statement of the multipolar expansion

The explicit solution to any linear elastic problem caused by a source internal to the medium is given by the representation

$$u_i(\mathbf{x}) = \int_{\mathbb{R}^3} G_{ij}(\mathbf{x} - \mathbf{x}') f^*_j(\mathbf{x}')\, \mathrm{d}\mathbf{x}', \tag{2.1}$$

where $i, j = 1, 2, 3$, repeated index denotes summation, $\mathrm{d}\mathbf{x} = \mathrm{d}x_1\mathrm{d}x_2\mathrm{d}x_3$ is the Cartesian measure, and u_i denotes the elastic displacement field, $G_{ij}(\mathbf{x})$ is the elastic Green's tensor,[1] and $f^*_j(\mathbf{x})$ denotes the elastic source term in its equivalent *Burridge–Knopoff* [47] force representation, which can be obtained from the eigenstrain representation of the inclusion as follows.

[1]For expressions in the elastic isotropic and anisotropic cases, see [23].

(i) Force representation of the inclusion

We will consider an inclusion $\mathcal{D}$ defined by the eigenstrain e^*_{il} constant for all $\mathbf{x} \in \mathcal{D}$. The Burridge–Knopoff theorem [47] states that for a source term defined by an eigenstrain e^*_{il}, the force representation is given by:

$$f^*_j(\mathbf{x}) = -\int_{\partial\mathcal{D}} C_{ikjl} e^*_{il} \delta(\mathbf{x} - \mathbf{x}') n_k \, \mathrm{d}S', \tag{2.2}$$

where C_{ijkl} is the elastic constant tensor, n_i is the surface normal vector, and $\delta(\mathbf{x})$ the delta function. For brevity, in the following we shall employ the equivalent eigenstress $\sigma^*_{kj} = C_{ikjl} e^*_{il}$ so that,

$$\begin{aligned} f^*_j(\mathbf{x}) &= -\int_{\partial\mathcal{D}} \delta(\mathbf{x} - \mathbf{x}') \sigma^*_{kj} n_k \, \mathrm{d}S' \\ &= -\int_{\mathcal{D}} \delta_k(\mathbf{x} - \mathbf{x}') \sigma^*_{kj} \, \mathrm{d}V' \\ &= -\sigma^*_{kj} \int_{\mathbb{R}^3} \delta_k(\mathbf{x} - \mathbf{x}') \chi_D(\mathbf{x}') \, \mathrm{d}V' = \sigma^*_{kj} \partial_k \chi_D(\mathbf{x}), \end{aligned} \tag{2.3}$$

where the divergence theorem and the fact that the system is homogeneous have been used. Here $\delta_k(\mathbf{x}) = \partial_k \delta(\mathbf{x})$ and $\chi_D(\mathbf{x})$ the characteristic function offering compact support on $\mathcal{D}$, i.e.

$$\chi_D(\mathbf{x}) = \begin{cases} 1 & \mathbf{x} \in \mathcal{D} \\ 0 & \mathbf{x} \notin \mathcal{D}. \end{cases} \tag{2.4}$$

Thus, we deduce that the ellipsoidal inclusion's force representation is given (in the sense of distributions) by:

$$f^*_j(\mathbf{x}) = C_{ikjl} e^*_{il} \partial_k \chi_D(\mathbf{x}). \tag{2.5}$$

We note that this formulation is entirely general, and holds for any inclusion $\mathcal{D}$ of any shape. Likewise, it is not limited to inclusions proper—the eigenstrain may represent an inhomogeneity [40] too.

(ii) Multipolar expansion of the external field of the inclusion

Knowledge of the force representation of the ellipsoidal inclusion (equations (2.5)) enables the explicit solution of its elastic field via the representation given in equations (2.1). The procedure to solve this problem analytically can be found e.g. in [7,8,23], and leads to a set of solutions dependent on elliptic integrals of the first and second kind which are famously complex when considering the external fields of the inclusion (cf. [48]). Rather, here we seek to approximate said solution via the multipolar expansion [29] of the representation formula equations (2.1).

To that end, we expand Green's tensor $G_{ij}(\mathbf{x} - \mathbf{x}')$ in Taylor series of $\mathbf{x}'$ about the origin:

$$G_{ij}(\mathbf{x} - \mathbf{x}') = \sum_{n=0}^{\infty} \frac{(-1)^n}{n!} \frac{\partial^n G_{ij}(\mathbf{x})}{\partial x_{k_1} \partial x_{k_2} \ldots \partial x_{k_n}} x'_{k_1} \cdot x'_{k_2} \cdot \ldots \cdot x'_{k_n} \tag{2.6}$$

and substitute this series expansion into the representation formula (equations (2.1)), whereupon

$$u_i(\mathbf{x}) = \int_{\mathbb{R}^3} f^*_j(\mathbf{x}') \sum_{n=0}^{\infty} \frac{(-1)^n}{n!} \frac{\partial^n G_{ij}(\mathbf{x})}{\partial x_{k_1} \ldots \partial x_{k_n}} x'_{k_1} \cdot \ldots \cdot x'_{k_n} \mathrm{d}\mathbf{x}' \tag{2.7}$$

$$= \sum_{n=0}^{\infty} \frac{(-1)^n}{n!} \frac{\partial^n G_{ij(\mathbf{x})}}{\partial x_{k_1} \ldots \partial x_{k_n}} \int_{\mathbb{R}^3} f^*_j(\mathbf{x}') x'_{k_1} \cdot \ldots \cdot x'_{k_n} \mathrm{d}\mathbf{x}' \tag{2.8}$$

$$= \sum_{n=0}^{\infty} \frac{(-1)^n}{n!} \frac{\partial^n G_{ij}(\mathbf{x})}{\partial x_{k_1} \ldots \partial x_{k_n}} \gamma^{(n)}_{jk_1,\ldots,k_n} \tag{2.9}$$

where $\gamma^{(n)}_{jk_1,\ldots,k_n}$ defines the nth-order multipolar moment of the force distribution f^*_j, and is represented by

$$\gamma^{(n)}_{jk_1,\ldots,k_n} = \int_{\mathbb{R}^3} f^*_j(\mathbf{x}')x'_{k_1} \cdot \ldots \cdot x'_{k_n}\,\mathrm{d}\mathbf{x}'. \tag{2.10}$$

Because the elastic Green's tensor itself decays with $1/r$, its nth-order derivative will decay with $1/r^{n+1}$, meaning that higher order terms in the multipolar expansion have increasingly small effect in the far field. As a result, with a few terms of the expansion it is possible to reach very accurate representations of the inclusion's elastic far field. Achieving this requires calculation of the multipolar moments $\gamma^{(n)}_{jk_1,\ldots,k_n}$, each of which is a number. We note that this same expansion can be achieved without using the Burridge–Knopoff force representation by operating with the Navier–Lamé equations in Fourier space.

(iii) Multipolar moments of the external field of the ellipsoidal inclusion

In order to compute the multipolar moment $\gamma^{(n)}_{jk_1,\ldots,k_n}$, we substitute the force representation of the ellipsoidal inclusion (equations (2.5)) into equations (2.10):

$$\gamma^{(n)}_{jk_1\ldots k_n} = \int_{\mathbb{R}^3} \sigma^*_{kj}x'_{k_1} \cdot \ldots \cdot x'_{k_n}\,\partial_k\chi_D(\mathbf{x}')\,\mathrm{d}\mathbf{x}' \tag{2.11}$$

$$= \sigma^*_{kj}\int_{\mathbb{R}^3} \pi_{k_1\ldots k_n}(\mathbf{x}')\partial_k\chi_D(\mathbf{x}')\,\mathrm{d}\mathbf{x}', \tag{2.12}$$

where the monomial

$$\pi_{k_1\ldots k_n}(\mathbf{x}') = x'_{k_1} \cdot \ldots \cdot x'_{k_n}, \tag{2.13}$$

is introduced for brevity. Using Green's identity and the fact that $\partial_k\chi_D(\mathbf{x})$ is likewise supported over $\mathcal{D}$, we can rework the integral above:

$$\gamma^{(n)}_{jk_1\ldots k_n} = \sigma^*_{kj}\int_{\mathcal{D}} \pi_{k_1\ldots k_n}(\mathbf{x}')\partial_k\chi_D(\mathbf{x}')\,\mathrm{d}\mathbf{x}' \tag{2.14}$$

$$= \sigma^*_{kj}\left[\int_{\partial\mathcal{D}} \pi_{k_1\ldots k_n}(\mathbf{x}')\chi_D(\mathbf{x}')n_k\,\mathrm{d}S' - \int_{\mathcal{D}} \frac{\partial\pi_{k_1\ldots k_n}(\mathbf{x}')}{\partial x'_k}\chi_D(\mathbf{x}')\,\mathrm{d}\mathbf{x}'\right] \tag{2.15}$$

$$= -\sigma^*_{kj}\int_{\mathcal{D}} \frac{\partial\pi_{k_1,\ldots,k_n}(\mathbf{x}')}{\partial x'_k}\,\mathrm{d}\mathbf{x}', \tag{2.16}$$

where the surface integral vanishes because $\chi_D(\mathbf{x}) = 0$ on the $\mathbf{x} \in \partial\mathcal{D}$.

Thus, in effect one is charged with computing integrals over the ellipsoid of a monomial of increasing order based on the selection of indices $k_1,\ldots,k_n$ and k. For low order moments, it is straightforward to list all possible resulting multipolar moments as we do in the sequel. However, as their order increases the number of possible multipolar moments increases with $C(n,3)$, so a systematic way of calculating all possible multipolar moments of the ellipsoidal inclusions becomes necessary. This is done in §2b and (c).

(b) Encoding of the indices

The integrand $\partial_k\pi_{k_1,\ldots,k_n}(\mathbf{x})$ of equations (2.16) depends on long permutations of the indices $k_1,k_2,\ldots,k_n,k$ with each index taking values $\{1,2,3\}$. Because the integrand is a monomial in $\mathbb{R}^3$, many different permutations will result in the same monomial in the integrand. For this reason, it is convenient to introduce the following encoding of the $k_1,\ldots,k_n,k$ indices:

$$i_p = \#(\partial_k\pi_{k_1\ldots k_n} \cap x_p) = \sum_{j=1}^{n}(\delta_{pk_j} - \delta_{kk_j}), \quad p = 1,2,3, \tag{2.17}$$

where i_p counts the number of times x_1 (for $p=1$), x_2 (for $p=2$) or x_3 (for $p=3$) appears in the monomial $\partial_k\pi_{k_1\ldots k_n}$. For further convenience, we collect the i_p in the multiindex $I = (i_1,i_2,i_3)$ with

$|I| = i_1 + i_2 + i_3$. Thus, we may write that the

$$\gamma^{(n)}_{jk_1\ldots k_n} = -(i_k + 1)\sigma^*_{kj}\gamma^I, \tag{2.18}$$

where

$$\gamma^I = \int_{\mathcal{D}} x_1^{i_1} x_2^{i_2} x_2^{i_2} \mathrm{d}\mathbf{x} = \int_{\mathcal{D}} \mathbf{x}^I \,\mathrm{d}\mathbf{x}, \tag{2.19}$$

and the $(i_k + 1)$ term accounts for the coefficient brought about the ∂_k derivative; if the term x_k is not present in the integrand, then $i_k = -1$, and hence $(i_k + 1)$ will cancel the multipolar moment, as required.

(c) General formula of the multipolar moment of an ellipsoidal inclusion

The highly symmetrical nature of the ellipsoid enables the obtention of closed-form general formulae for all multipolar moments of arbitrary order. Here we report directly the general result and some useful intermediate ones, with their general derivation given in electronic supplementary material. For brevity, here we quote the main results directly.

Thus, denote a general multiindex $I = (i_p, i_q, i_r)$ with $p \neq q \neq r \in \{1, 2, 3\}$. Then, when $m = n - 1 > 0$ and $I = (m, 0, 0)$:

$$\gamma^{(m,0,0)} = \frac{2(1 + (-1)^m)}{(m + 1)(m + 3)} \pi a_p^{m+1} a_q a_r. \tag{2.20}$$

The term $(1 + (-1)^m)/2$ is introduced to capture the fact that the multipolar moments of even order are zero.

When $m + k = n - 1$ and $I = (m, k, 0)$:

$$\gamma^{(m,k,0)} = \frac{(1 + (-1)^m)(1 + (-1)^k)\Gamma((m + 1)/2)\Gamma((k + 1)/2)}{2(m + k + 3)\Gamma((1/2)(n + 2))} \sqrt{\pi} a_p^{m+1} a_q^{k+1} a_r, \tag{2.21}$$

where $\Gamma(z)$ is the Gamma function.

Finally, the general formula when $m + k + w = n - 1$ and accordingly $I = (m, k, w)$:

$$\gamma^{(m,k,w)} = \frac{(1 + (-1)^m)(1 + (-1)^k)(1 + (-1)^w)\Gamma((m + 1)/2)\Gamma((k + 1)/2)\Gamma((w + 1)/2)}{4(n + 2)\Gamma((1/2)(n + 2))} a_p^{m+1} a_q^{k+1} a_r^{w+1}. \tag{2.22}$$

This completes the derivation of all possible multipolar moments of the ellipsoidal inclusion. Table S1 in electronic supplementary material collects some of the low-order multipolar moments. All other higher order moments may be obtained by combining equation (2.18) with equation (2.22).

(d) The far field and the near field

The multipolar field expansion of an ellipsoidal inclusion can therefore be reduced to:

$$u_i(\mathbf{x}) = \sum_{n=0}^{\infty} \gamma^{(2n+1)}_{jk_1k_2\ldots k_{2n+1}} \frac{\partial^{(2n+1)} G_{ij}}{\partial x_{k_1} \partial x_{k_2} \ldots \partial x_{k_{2n}} \partial x_{k_{2n+1}}}. \tag{2.23}$$

The stress fields follow naturally from the displacement field expansion as:

$$\sigma_{il}(\mathbf{x}) = \sum_{n=0}^{\infty} \gamma^{(2n+1)}_{jk_1k_2\ldots k_{2n}} C_{ilpq} \frac{\partial^{(2n+1)} G_{pj}}{\partial x_q \partial x_{k_1} \partial x_{k_2} \ldots \partial x_{k_{2n}} \partial x_{k_{2n+1}}}, \tag{2.24}$$

which in the isotropic case reduces to

$$\sigma_{il}(\mathbf{x}) = \sum_{n=0}^{\infty} \gamma^{(2n+1)}_{jk_1,k_2,\ldots,k_{2n+1}} [\lambda \delta_{il} G_{pj,pk_1\ldots k_{2n+1}} + 2\mu G_{ij,lk_1\ldots k_{2n+1}}]. \tag{2.25}$$

Equation (2.23)–(2.25) are general, and apply to any inclusion (or inhomogeneity) irrespective of its shape. When truncated to dipolar order, we would find that

$$u_i^{(1)}(\mathbf{x}) = \frac{4}{3}\pi a_1 a_2 a_3 \sigma^*_{jk_1} G_{ij,k_1} = V(\lambda \delta_{jk_1} e^*_{pp} + 2\mu e^*_{jk_1})\, G_{ij,k_1}, \tag{2.26}$$

where $V = (4/3)\pi a_1 a_2 a_3$ is the volume of the ellipsoid, and Green's function first derivative can be expressed as [23]

$$G_{ij,k_1} = \frac{1}{16\pi(1-\nu)\mu}\frac{1}{r^2}[(3-4\nu)\rho_{k_1}\delta_{ij} - \rho_j\delta_{jk_1} - \rho_i\delta_{jk_1} + 3\rho_i\rho_j\rho_k], \tag{2.27}$$

with $\rho_i = x_i/r$, $r = |\mathbf{x}|$ is the direction cosine along x_i, whereupon we might collect the numerator terms as:

$$g_{ijk_1} = (1-2\nu)(\rho_{k_1}\delta_{ij} + \rho_j\delta_{ik_1} - \rho_i\delta_{jk_1}) + 3\rho_i\rho_j\rho_{k_1}, \tag{2.28}$$

so that we recover of Eshelby's formula for the point defect (see eqn. (2.23) in [40]), namely that

$$u_i^{(1)}(\mathbf{x}) = \frac{Ve^*_{jk_1}}{8\pi(1-\nu)r^2} g_{ijk_1}. \tag{2.29}$$

Thus, the fact that all dipolar moments of an ellipsoidal inclusion depend solely on their volume may be understood as the fact that from afar, all inclusions behave like point defects. The dipolar elastic field also shows that the far field of the inclusion will be dominated by $1/r^2$ terms, and that their stress field will therefore decay with $1/r^3$. This serves to verify that the multipolar field expansion mirror behaviour deduced from the exact fields of the ellipsoidal inclusion.

However, the multipolar expansion also showcases the extent to which the inclusion behaves as a point defect in its far field, as it provides us with a *lengthscale* with which to evaluate the range of each successive multipolar term. For any inclusion, the dipolar terms entail a $1/r^2$ decay, and so long as the inclusion is ellipsoidal, the next non-vanishing multipole, the octopolar term (see equation (2.22)), entails a $1/r^4$ decay. Then, we may define the depth α for the far field as the distance from the ellipsoid's centroid beyond which the dipolar contributions dominate the far field. This is achieved by comparing the magnitude of the dipolar and octopolar moments themselves:

$$\alpha_j > \max\sqrt{\left[\frac{\gamma^{(3)}_{jk_1k_2k_3}}{\gamma^{(1)}_{jk_1}}\right]} \propto \max a_j. \tag{2.30}$$

This means that in each spatial direction x_j, the near-field's effects are expected to become dominant only for distances smaller than about the largest axis of the ellipsoid. This entails that whereas eqn. 2.29 does capture the far field of the ellipsoidal inclusion, its applicability is directional. For example, long and thin inclusions (shear zones, martensites) will resemble point defects in the far field more strongly in the direction in which they are thin than in the direction in which they are long, and this discrepancy can be corrected by considering additional higher order multipolar terms, which can be readily evaluated at a fraction of the cost of the full-field expansion.

Likewise, the ratio between octopolar and dodecapolar moments would provide the next lengthscale in the near field:

$$\beta_j > \sqrt{\left[\frac{\gamma^{(5)}_{jk_1k_2k_3k_4k_4}}{\gamma^{(3)}_{jk_1k_2k_3}}\right]} \propto \sqrt{\frac{3}{7}}\max a_j. \tag{2.31}$$

The quantities α_j, β_j offer an upper bound to the convergence of the multipolar terms, and are otherwise affected by specific orientations. Still, they highlight how the far field is dominated by dipolar terms, and the near field by octopolar terms: all further contributions concern lengthscales smaller than the geometric dimensions of the inclusion itself. This rate of convergence is depicted in figure 2, which shows the evolution of the first three multipolar stress components of an ellipsoidal inclusion of dimensions $a_1 = 0.25\,\mathrm{m}$, $a_2 = 0.2\,\mathrm{m}$, $a_3 = 0.175\,\mathrm{m}$; as can be seen, the far

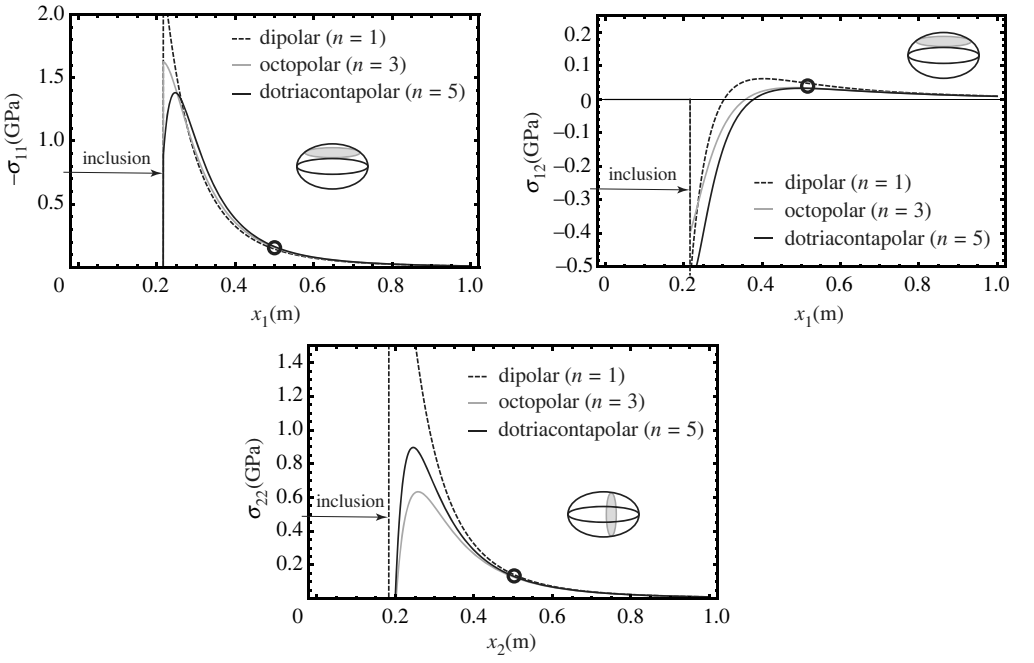

Figure 2. Multipolar stress field components for an ellipsoidal inclusion of dimensions $a_1 = 0.25$ m, $a_2 = 0.2$ m, $a_3 = 0.175$ m, defined by shear zone of $e^*_{12} = 1$ (and all other eigenstrain components zero), in a material with $\mu = 1$ GPa, $\nu = 0.33$. For σ_{11} and σ_{12}, the stress field on the line ($x_2 = 0.1, x_3 = 0$) m is shown; for σ_{22}, on the line ($x_1 = 0.1, x_3 = 0$) m.

field is accurately captured at a distance away from the inclusion of about $|\mathbf{x}| > a_1 = 0.25$ m, beyond which all three terms converge to the dipolar, long-range field. Figure 3 in turn offers a complete representation of the multipolar stress field components in the plane, comparing them to the exact solution (found e.g. in [23], ch. 2). As can be seen, the basic, long-range features of stress fields are appropriately captured at dipolar order, and higher order approximations approximate with increasing accuracy the near-field features of the exact solution, from a distance of about the length of its axes.

3. Polytopal inclusions

The ellipsoidal inclusion serves to model a vast number of defects of micromechanical and macroscopic concern: from twins and martensitic needles [3] to shear zones in tectonics [1]. However, in some circumstances (particularly, but not exclusively, if the material is anisotropic), inclusions display characteristic faceting and may be construed to be polytopes, i.e. made up by vertices, edges and facets. Polytopal inclusions are of particular interest in, among others, the study of igneous and metamorphic aggregates in rocks, the study of particle reinforced composites, the study of precipitates in metallic alloys, and in quantum dots in semiconductors. In rocks, faceted phenocrysts and groundmass of 'polygonal' [2] shapes are typical. Likewise, they are typical in metallic alloys, when intermetallic phases are present (e.g. spinel formation in steels [49]), which has warranted in the past extensive studies of the cuboidal inclusion [9] and varied polytopal geometries (e.g. stars [50]). Likewise, polytopal inclusions in anisotropic quantum dot crystals can be employed, through their elastic fields, to tune quality of the photons emitted by the quantum dots has led to considerable efforts aimed at describing the elastic fields of polytopal inclusions [6,20,51,52], often leading to intricate solutions [51,52]. Finally, polytopal inclusions are of interest as approximations to more complex geometries: given an inclusion of surface $\partial\mathcal{D}$, it is always possible to approximate it via surface triangulation [53].

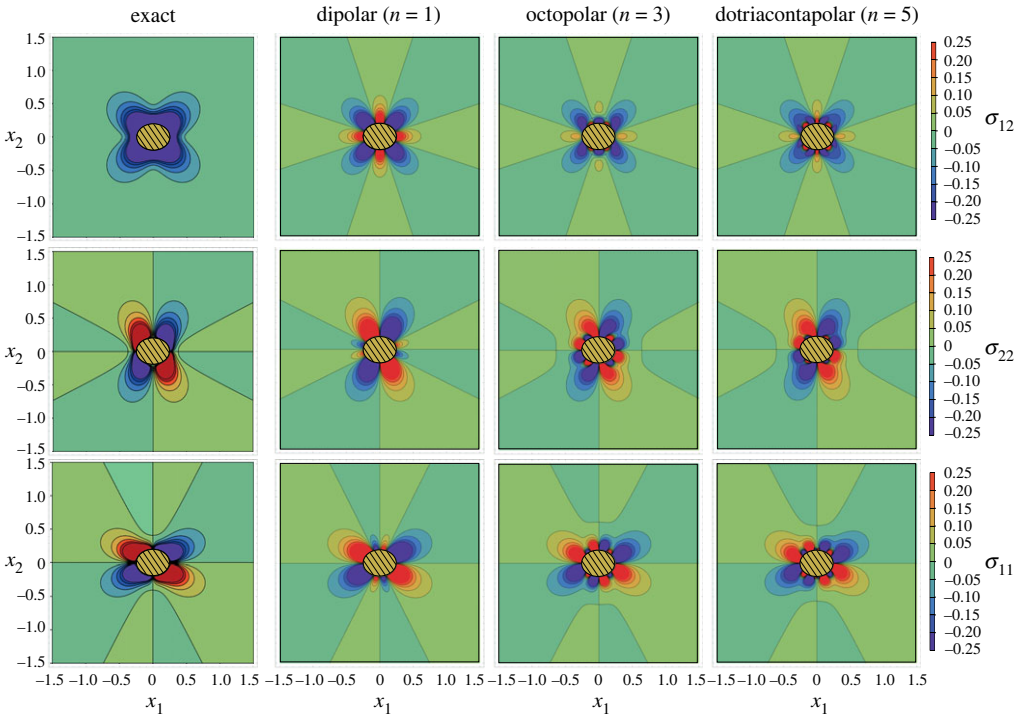

Figure 3. Exact and multipolar stress field components (in GPa) for an ellipsoidal inclusion of dimensions $a_1 = 0.25$ m, $a_2 = 0.2$ m, $a_3 = 0.175$ m, defined by a shear zone of $e^*_{12} = 1$ (all other eigenstrain components zero), with $\mu = 1$ GPa, $\nu = 0.33$. The lengthscale and elastic constants are merely representative; in the electronic supplementary material a Mathematica notebook is provided to enable the computation of the multipolar fields of inclusions with any desired combination of elastic constants and dimensions.

(a) General expression of the multipolar moments of an inclusion

The procedure outlined in §2 to derive the multipolar field expansion of the elastic fields of an ellipsoidal inclusion can be applied to any other inclusion, provided the force representation is known. This is because the Taylor series expansion leading to equation (2.9) is valid so long as the force representation $f_j(\mathbf{x})$ remains a measurable function, which ought to be the case since the inclusion thus represented necessarily exists (at least at the atomistic level) as an energy minimum configuration in a conservative field (cf. [3]). Thus, irrespective of the geometry of the inclusion, the multipolar moments themselves will still be given by equation (2.10):

$$\gamma^{(n)}_{jk_1,\ldots,k_n} = \int_{\mathbb{R}^3} x'_{k_1} \cdot \ldots \cdot x'_{k_n} \cdot f^*_j(\mathbf{x}')\,\mathrm{d}\mathbf{x}', \tag{3.1}$$

where in this case $f^*_j(\mathbf{x}')$ is the force representation.

Let us assume that the inclusion is some closed shape $\mathcal{P}$ of constant eigenstrain e^*_{ij} inside, or, equivalently, of constant eigenstress σ^*_{kj}. Then its force representation will be:

$$f^*_j(\mathbf{x}) = \sigma^*_{kj}\partial_k \chi_P(\mathbf{x}), \tag{3.2}$$

where $\chi_P(\mathbf{x})$ is the characteristic function of the inclusion. We note that the force representation induces a measure μ_P, namely

$$\mu_P(\mathbf{x}) = \chi_P(\mathbf{x}), \tag{3.3}$$

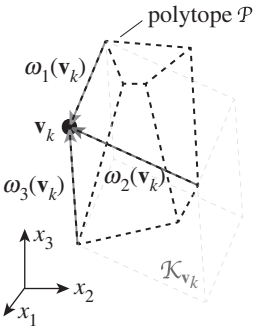

Figure 4. Schematic of a general convex, simple polytope $\mathcal{P}$ in $\mathbb{R}^3$. The polytope is represented with dashed black lines. Over the vertex v_k, the three incident vectors $\omega_1(\mathrm{v}_k)$, $\omega_2(\mathrm{v}_k)$, $\omega_3(\mathrm{v}_k)$ are shown, forming a tangent cone; the parallelepiped $\mathcal{K}_{\mathrm{v}_k}$ formed by the three incident vectors is shown in dashed grey lines.

so that the multipolar moments are

$$\gamma^{(n)}_{jk_1,\ldots,k_n} = -\sigma^*_{kj}\int_{\mathbb{R}^3} \pi_{k_1\ldots k_n,k}(\mathbf{x})\,\mathrm{d}\mu_P(\mathbf{x}'). \tag{3.4}$$

As in the case of the ellipsoidal inclusion, in light of the monomial $\pi_{k_1\ldots k_n,k}(\mathbf{x})$ it is convenient to encode the indices $k_1,\ldots,k_n,k$ into the multiindex $I=(i_1,i_2,i_3)$ given by equation (2.17), so that

$$\left.\begin{aligned}\gamma^{(n)}_{jk_1\ldots k_n} &= -\sigma^*_{kj}(i_k+1)\gamma^I\\ \text{and}\qquad \gamma^I \equiv \gamma^{(i_1,i_2,i_3)} &= \int_{\mathbb{R}^3} x_1^{i_1}x_2^{i_2}x_3^{i_3}\,\mathrm{d}\mu_P(\mathbf{x}).\end{aligned}\right\} \tag{3.5}$$

(b) Moments of a polytope: representation of a convex polytope in three dimensions

In three dimensions, a polytope is a polyhedron made up of vertices and planar facets. Clearly, the computation of the integral equation (3.5) for a general polytope P of numerous facets and vertices will be particularly cumbersome (cf. [51]) unless some general mathematical theory able to offer general procedures with which to integrate over multiple edges and faces of arbitrary polytopes is employed. Here we employ recent developments in integer-point enumeration theory, stemming from geometric combinatorics (cf. [41]), to that end, deriving a general algorithm for calculating all possible moments of a given simple polytope. This will rely on the cone decomposition of the polytope at its vertices, which we describe in the sequel.

(i) Cone decomposition of a polytope

We will consider a general convex, simple polytope such as that depicted in figure 4, which we denote by $\mathcal{P}\subset\mathbb{R}^3$. $\mathcal{P}$ is defined by N vertices $\{\mathbf{v}_k\}_{k=1}^N$. For brevity, we call the set of all vertices as $\mathcal{V}=(\mathbf{v}_1,\mathbf{v}_2,\ldots,\mathbf{v}_N)$. Since the polytope is simple and we operate in $\mathbb{R}^3$, over each vertex $\mathbf{v}_k$ there meet three edges. We define the edge vectors of the vertex $\mathbf{v}_k$ as the three vectors $\omega_1(\mathbf{v}_k)$, $\omega_2(\mathbf{v}_k)$, $\omega_3(\mathbf{v}_k)$ parallel to each edge incident on the vertex $\mathbf{v}_k$. The positive span of these three edge vectors forms a cone $\mathcal{K}_{\mathbf{v}_k}$, known as the *tangent cone* $\mathcal{K}_{\mathbf{v}}=\{a_1\omega_1(\mathbf{v})+a_2\omega_2(\mathbf{v})+a_3\omega_3(\mathbf{v}) : a_1,a_2,a_3\geq 0\}\subset\mathbb{R}^3$. We denote by $|\det\mathcal{K}_{\mathbf{v}_k}|$ the volume of the parallelepiped formed by the edge vectors $\omega_1(\mathbf{v}_k)$, $\omega_2(\mathbf{v}_k)$, $\omega_3(\mathbf{v}_k)$, that is, $|\det(\omega_1(\mathbf{v}_k),\omega_3(\mathbf{v}_k),\omega_3(\mathbf{v}_k))|$.

(ii) Brion's formula for the moments of a convex polytope

With those definitions in place, it is possible to calculate the general moment γ_I (equation (3.5)) of a simple polytope in at least three complementary ways. The first can be found in §12.3 (pp. 218–220) of [41]. It relies on the continuous form of Brion's theorem [54] over simple, rational,

convex polytopes, later generalized to any convex polytope by Barvinok [55]. According to Brion's theorem, the integral of $e^{\mathbf{x}\cdot\mathbf{u}}$ over the polytope $\mathcal{P}$ is given by:

$$\int_{\mathbb{R}^3} e^{\mathbf{x}\cdot\mathbf{u}} \mathrm{d}\mu_P(\mathbf{x}) = -\sum_{\mathbf{v}_k\in\mathcal{V}} \frac{e^{\mathbf{v}_k\cdot\mathbf{u}}|\det\mathcal{K}_{\mathbf{v}_k}|}{(\omega_1(\mathbf{v}_k)\cdot\mathbf{u})(\omega_2(\mathbf{v}_k)\cdot\mathbf{u})(\omega_3(\mathbf{v}_k)\cdot\mathbf{u})}. \tag{3.6}$$

Now we consider the following integral, for the multiindex $I = (i_1, i_2, i_3)$:

$$\begin{aligned}\int_{\mathcal{P}} \mathbf{x}^I e^{\mathbf{x}\cdot\mathbf{u}}\,\mathrm{d}\mathbf{x} &= \int_{\mathcal{P}} \left(\frac{\partial}{\partial\mathbf{u}}\right)^I e^{\mathbf{x}\cdot\mathbf{u}}\mathrm{d}\mathbf{x} \\ &= -\left(\frac{\partial}{\partial\mathbf{u}}\right)^I \left[\sum_{\mathbf{v}_k\in\mathcal{V}} \frac{e^{\mathbf{v}_k\cdot\mathbf{u}}|\det\mathcal{K}_{\mathbf{v}_k}|}{(\omega_1(\mathbf{v}_k)\cdot\mathbf{u})(\omega_2(\mathbf{v}_k)\cdot\mathbf{u})(\omega_3(\mathbf{v}_k)\cdot\mathbf{u})}\right].\end{aligned} \tag{3.7}$$

Thus, in the limit when $\mathbf{u}\to 0$, the integral above becomes the moment integral, whereupon

$$\gamma^I = \int_{\mathcal{P}} \mathbf{x}^I \mathrm{d}\mathbf{x} = -\lim_{\mathbf{u}\to 0}\left(\frac{\partial}{\partial\mathbf{u}}\right)^I \sum_{\mathbf{v}_k\in\mathcal{V}} \left[\frac{e^{\mathbf{v}_k\cdot\mathbf{u}}|\det\mathcal{K}_{\mathbf{v}_k}|}{(\omega_1(\mathbf{v}_k)\cdot\mathbf{u})(\omega_2(\mathbf{v}_k)\cdot\mathbf{u})(\omega_3(\mathbf{v}_k)\cdot\mathbf{u})}\right] = -\lim_{\mathbf{u}\to 0}\left(\frac{\partial}{\partial\mathbf{u}}\right)^I V(\mathbf{u}), \tag{3.8}$$

where for brevity we name:

$$V(\mathbf{u}) = \sum_{\mathbf{v}_k\in\mathcal{V}} \left[\frac{e^{\mathbf{v}_k\cdot\mathbf{u}}|\det\mathcal{K}_{\mathbf{v}_k}|}{(\omega_1(\mathbf{v}_k)\cdot\mathbf{u})(\omega_2(\mathbf{v}_k)\cdot\mathbf{u})(\omega_3(\mathbf{v}_k)\cdot\mathbf{u})}\right]. \tag{3.9}$$

(c) General algorithm for the calculation of the moments of a convex polytope of any order

Equation (3.8), found in [41], suffices to compute all desired moments of a polytope. It is however computationally cumbersome, as it involves the derivatives of exponential functions and the computation of a limit. For this reason, in what follows we will derive a more computationally effective alternative general formula for the moments of the polytope.

We achieve this by manipulating theorem 12.4 of [41], originally due to Brion and Vergne (theorem 3.2 in [56], also found in e.g. [41,57]), which in its original form concerns the volume and the axial moment function of the polytope $\mathcal{P}$. According to said theorem, we begin by considering Brion's theorem (equation (3.6)), and note that we may re-scale the $\mathbf{u}$ variable into $\mathbf{u}\mapsto s\mathbf{z}$, with $s\in\mathbb{R}$. Having done this, we then expand the integral on Brion's theorem (equation (3.6)) in Taylor series of the scaling factor s about the origin:

$$\int_{\mathcal{P}} e^{\mathbf{x}\cdot s\mathbf{z}}\mathrm{d}\mathbf{x} = \sum_{j=0}^{\infty}\left[\int_{\mathcal{P}} (\mathbf{x}\cdot\mathbf{z})^j\,\mathrm{d}\mathbf{x}\right]\frac{s^j}{j!}, \tag{3.10}$$

where now the series expansion depends on the axial moment function:

$$\gamma^{(j)}(\mathbf{z}) = \int_{\mathcal{P}} (\mathbf{x}\cdot\mathbf{z})^j\,\mathrm{d}\mathbf{x}. \tag{3.11}$$

If we proceed likewise with the r.h.s. of equation (3.6), we get

$$\begin{aligned}&-\sum_{\mathbf{v}_k\in\mathcal{V}} \frac{e^{s(\mathbf{v}_k\cdot\mathbf{z})}|\det\mathcal{K}_{\mathbf{v}_k}|}{(s^3\omega_1(\mathbf{v}_k)\cdot\mathbf{z})(\omega_2(\mathbf{v}_k)\cdot\mathbf{z})(\omega_3(\mathbf{v}_k)\cdot\mathbf{z})} \\ &= -\sum_{j=-3}^{\infty}\left[\sum_{\mathbf{v}_k\in\mathcal{V}} (\mathbf{v}_k\cdot\mathbf{z})^{j+3}\frac{|\det\mathcal{K}_{\mathbf{v}_k}|}{(\omega_1(\mathbf{v}_k)\cdot\mathbf{z})(\omega_2(\mathbf{v}_k)\cdot\mathbf{z})(\omega_3(\mathbf{v}_k)\cdot\mathbf{z})}\right]\frac{s^j}{(j+3)!}.\end{aligned} \tag{3.12}$$

Comparing both sides of the equation term-by-term, we find that the axial moment function $\gamma^{(j)}(\mathbf{z})$ may be expressed as:

$$\begin{aligned}\gamma^{(j)}(\mathbf{z}) &= \int_{\mathcal{P}} (\mathbf{x}\cdot\mathbf{z})^j \,\mathrm{d}\mathbf{x} \\ &= -\frac{j!}{(j+3)!}\sum_{\mathbf{v}_k\in\mathcal{V}} (\mathbf{v}_k\cdot\mathbf{z})^{j+3}\frac{|\det\mathcal{K}_{\mathbf{v}_k}|}{(\omega_1(\mathbf{v}_k)\cdot\mathbf{z})(\omega_2(\mathbf{v}_k)\cdot\mathbf{z})(\omega_3(\mathbf{v}_k)\cdot\mathbf{z})}.\end{aligned} \tag{3.13}$$

Clearly, $\gamma^{(j)}(\mathbf{z})$ is not a moment proper (it depends on $\mathbf{z}$), nor one we are necessarily interested in, as its index is an integer. If $\mathbf{z}$ were one of the three unit vectors, then $\gamma^{(j)}(\mathbf{z})$ can be used to select the axial moments of order j, e.g.:

$$\gamma^{(j)}(1,0,0) = \int_{\mathcal{P}} x_1^j \,\mathrm{d}\mathbf{x} \equiv \gamma^{(j,0,0)}. \tag{3.14}$$

However, what we seek is γ^I, with I the multiindex $I=(i_1,i_2,i_3)$ encoding the $k_1\ldots k_nk$ indices in the multipolar moments. Here we show how a few simple manipulations of the axial moment function $\gamma^{(j)}(\mathbf{z})$ enables us to relate this result by Brion and Vergne to the desired moments γ^I. Indeed, we may expand the axial moment function $\gamma^{(j)}(\mathbf{z})$ in series of $\mathbf{z}$ about the origin, where we use again the multiindex $I=(i_1,i_2,i_3)$ for convenience:

$$\gamma^{(j)}(\mathbf{z}) = \sum_{|I|\geq 0}\frac{\mathbf{z}^I}{|I|!}\left(\frac{\partial}{\partial\mathbf{z}}\right)^I \gamma^{(j)}(\mathbf{z})\bigg|_{\mathbf{z}=0}. \tag{3.15}$$

This series is capped at $|I|=j$, as higher-order derivatives vanish in the integrand.

Likewise, we can expand $\gamma^{(j)}(\mathbf{z})$ itself in powers $(\mathbf{x}\cdot\mathbf{z})^j$ via the multinomial sum:

$$(\mathbf{x}\cdot\mathbf{z})^j = (x_1z_1+x_2z_2+x_3z_3)^j = \sum_{|I|=j}\binom{j}{I}\mathbf{x}^I\mathbf{z}^I, \tag{3.16}$$

where

$$\binom{j}{I} = \binom{j}{i_1,i_2,i_3} = \frac{j!}{i_1!\,i_2!\,i_3!}, \tag{3.17}$$

so that

$$\int_{\mathcal{P}}(\mathbf{x}\cdot\mathbf{z})^j\,\mathrm{d}\mathbf{x} = \sum_{|I|=j}\binom{j}{I}\mathbf{z}^I\int_{\mathcal{P}}\mathbf{x}^I\,\mathrm{d}\mathbf{x} = \sum_{|I|=j}\binom{j}{I}\mathbf{z}^I\gamma^I. \tag{3.18}$$

Now, if we group the terms in the Taylor series so that $|I|=j$, we can compare them to the terms in the multinomial series, and conclude that the desired γ^I moments of the general polytope $\mathcal{P}$ can be represented via

$$\gamma^I = \frac{1}{|I|!}\left(\frac{\partial}{\partial\mathbf{z}}\right)^I \gamma^{|I|}(\mathbf{z})\bigg|_{\mathbf{z}=0}, \tag{3.19}$$

where

$$\gamma^{|I|}(\mathbf{z}) = -\frac{|I|!}{(|I|+3)!}\sum_{\mathbf{v}_k\in\mathcal{V}}(\mathbf{v}_k\cdot\mathbf{z})^{|I|+3}\frac{|\det\mathcal{K}_{\mathbf{v}_k}|}{(\omega_1(\mathbf{v}_k)\cdot\mathbf{z})(\omega_2(\mathbf{v}_k)\cdot\mathbf{z})(\omega_3(\mathbf{v}_k)\cdot\mathbf{z})}, \tag{3.20}$$

where naturally $|I|\equiv j$.

Equation (3.19) relates the axial moment function $\gamma^{|I|}(\mathbf{z})$ to all other moments of the polytope. Analytically, this is advantageous because the axial moment function does not include exponential terms, and the formula involves only derivatives rather than limits of derivatives, resulting in a computationally simpler way of obtaining the desired moments of the polytope. A third, alternative formulation reliant on the moment generating function of a convex polytope can be found in [58], and is provided in the electronic supplementary material.

Further, equation (3.19) provides an efficient algorithm to compute any multipolar moment of a polytope: (1) for a given order $|I|$, obtain the axial moment function $\gamma^{|I|}(\mathbf{z})$ (equation (3.20)); (2) calculate the desired multipolar moment γ^I using equation (3.19). The electronic

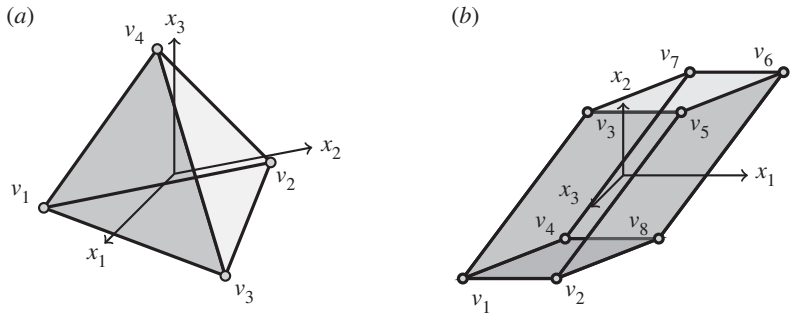

Figure 5. Two polytopal inclusions. (*a*) Tetrahedral inclusion. (*b*) Cuboidal inclusion.

supplementary material provides an example on how to operate with the axial moment function formula derived here.

(d) Tetrahedral inclusion

We consider the tetrahedral inclusion $\mathcal{V}$ (a 3-simplex) shown in figure 5*a*. The tetrahedron has height of magnitude f, sides of size a, $\sqrt{b^2+c^2}$, and $\sqrt{d^2+e^2}$. We place the vertices in such a manner that the centroid of the tetrahedron falls at the origin: $\mathbf{v}_1 = -(1/4)(a+b+c, c+e, f)$, $\mathbf{v}_2 = (a-(1/4)(a+b+d), -(1/4)(c+e), -(1/4)f)$, $\mathbf{v}_3 = (b-(1/4)(a+b+d), c-(1/4)(c+e), -(f/4))$, $\mathbf{v}_4 = (d-(1/4)(a+b+d), e-(1/4)(c+e), (3f/4))$. We define the edge vectors as $\boldsymbol{\omega}_i(\mathbf{v}_k) = \mathbf{v}_i - \mathbf{v}_k$, $i = \{n \in \{1,2,3,4\} : i \neq k\}$, and using equation (3.19), we find that the axial moment function is:

$$\gamma^{(j)}(\mathbf{u}) = -\frac{j!}{(j+3)!}\frac{|acf|}{4^{j+3}}\left(-\frac{(-au_1-bu_1-cu_2+3du_1+3eu_2+3fu_3)^{j+3}}{(du_1+eu_2+fu_3)(-au_1+du_1+eu_2+fu_3)(-bu_1-cu_2+du_1+eu_2+fu_3)}+\right.$$
$$+\frac{(-au_1-bu_1-cu_2-du_1-eu_2-fu_3)^{j+3}}{au_1(bu_1+cu_2)(du_1+eu_2+fu_3)}+\frac{(3au_1-bu_1-cu_2-du_1-eu_2-fu_3)^{j+3}}{au_1(au_1-bu_1-cu_2)(-au_1+du_1+eu_2+fu_3)}-$$
$$\left.-\frac{(-au_1+3bu_1+3cu_2-du_1-eu_2-fu_3)^{j+3}}{(bu_1+cu_2)(-au_1+bu_1+cu_2)(bu_1+cu_2-du_1-eu_2-fu_3)}\right) \tag{3.21}$$

The axial moment function enables us to generate all other multipolar moments of the inclusion via equation (3.19). Table S2 in the electronic supplementary material collects them up to third order. Figure 6 depicts the hydrostatic stress component on the cross-section afforded by the lower face of two distinct tetrahedra of the same volume, one symmetric in the x_2 and the other skewed. The hydrostatic stress field is chosen in order to diminish the difficulties posed by having to rotate the stress tensor, particularly when the polytope is skewed or rotated about the origin. As has been discussed, all long-range interactions depend solely on the dipolar terms, which are proportional to the volume of the tetrahedron alone. And indeed, as is shown in figure 6*a*,*b*, because both tetrahedra have the same volume, the long-range fields of both tetrahedra are the same, irrespective of the shape (and orientation) of the inclusion. Further, they are homologous with those of the ellipsoidal inclusion, and indeed to those of the point defect, and given by (for the case represented in figure 6):

$$\sigma_h^{(1)}(\mathbf{x}) = -\frac{\mu(1+\nu)x_1x_2}{\pi(1-\nu)r^{5/2}}Ve_{12}^*, \tag{3.22}$$

where V is the polytope's volume. The effect of shape is only felt in the near fields: with the octopolar contributions, short range effects start to be accounted for: the skewed tetrahedron's hydrostatic field in figure 6*b* becomes increasingly asymmetrical in its near field, something not observed in the symmetric tetrahedron shown in figure 6*a*. This becomes increasingly

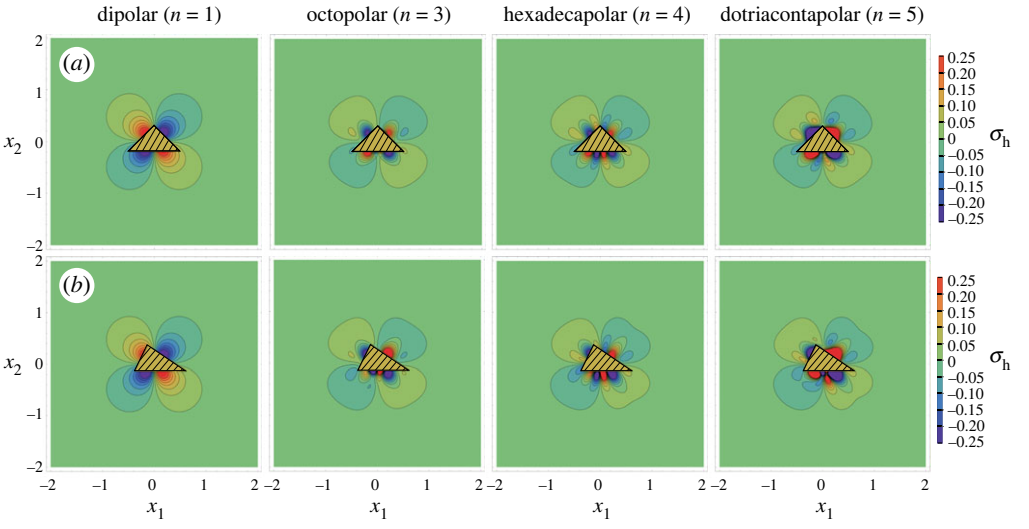

Figure 6. The hydrostatic stress field (in GPa) of a nominal tetrahedral inclusion. Two equivoluminal tetrahedra are considered: *a*, defined by the set of vertices (−1/2, −3/16, −1/4), (1/2, −3/16, −1/4), (0, 5/16, −1/4), (0, 1/16, 3/4); and *b* by the vertices (−0.375, −0.1375, −0.25), (0.625, −0.1375, −0.25), (−0.125, 0.3625, −0.25), (−0.125, −0.0875, 0.75) (all units in m), with the origin placed at the centroid of the corresponding tetrahedron. The inclusion is defined as zone of constant given by the eigenstrain $e^*_{12} = 1$ (all other eigenstrain components zero). The figure depicts the cross-section of the field on the lower face of the tetrahedra (for both *a* and *b*, $x_3 = -0.25$ m), i.e. on the lower face of the tetrahedron, embedded in a material with $\mu = 1$ GPa, $\nu = 0.33$.

more marked as the order of the expansion increases. We note here that because the origin of coordinates is placed at the centroid, the quadrupolar moments vanish and their associated field is exactly the dipolar one; but because the tetrahedron lacks ellipsoidal symmetry, the hexadecapolar moments do not vanish and contribute to the near field. This means that the near field contribution is unlike that of the ellipsoidal inclusion; this is generally the case for all polytopes, and has considerable implications for the nature of the short-range fields of polytopal inclusions, as we discuss further in §3g.

(e) Cuboidal inclusion

A general cuboidal inclusion $\mathcal{V}$ can be represented by the parallelepiped shown in figure 5*b*. We choose to place the vertices at $\mathbf{v}_1 = (0,0,0)$, $\mathbf{v}_2 = (a,0,0)$, $\mathbf{v}_3 = (c,d,0)$, $\mathbf{v}_4 = (e,f,g)$, $\mathbf{v}_5 = (a+c,d,0)$, $\mathbf{v}_6 = (a+c+e,d+f,g)$, $\mathbf{v}_7 = (c+e,d+f,g)$, $\mathbf{v}_8 = (a+e,f,g)$. This places the centroid at $\mathbf{v}_c = ((1/2)(a+c+e),(1/2)(d+f),(g/2))$. For cancellation purposes, we relocate the origin to the centroid, so that now all vertices can be found at $\mathbf{v}_k \mapsto \mathbf{v}_k - \mathbf{v}_c$. The edge vectors $\boldsymbol{\omega}_i(\mathbf{v}_k)$ are defined as the incident sides over each vertex shown in figure 5*b*, e.g. $\omega_1(\mathbf{v}_1) = \mathbf{v}_2 - \mathbf{v}_1, \omega_2(\mathbf{v}_1) = \mathbf{v}_3 - \mathbf{v}_1, \omega_3(\mathbf{v}_1) = \mathbf{v}_4 - \mathbf{v}_1$, etc. This results in the following axial moment:

$$\begin{aligned}\gamma^{(j)}(\mathbf{u}) = \frac{|adg|}{2^{j+3}au_1(cu_1+du_2)(eu_1+fu_2+gu_3)}[&-(-au_1+cu_1+du_2+eu_1+fu_2+gu_3)^{j+3}\\ &+(au_1+cu_1+du_2+eu_1+fu_2+gu_3)^{j+3}+(-au_1-cu_1-du_2+eu_1+fu_2+gu_3)^{j+3}\\ &-(au_1-cu_1-du_2+eu_1+fu_2+gu_3)^{j+3}+(-au_1+cu_1+du_2-eu_1-fu_2-gu_3)^{j+3}\\ &-(au_1+cu_1+du_2-eu_1-fu_2-gu_3)^{j+3}-(-au_1-cu_1-du_2-eu_1-fu_2-gu_3)^{j+3}\\ &+(au_1-cu_1-du_2-eu_1-fu_2-gu_3)^{j+3}]\end{aligned} \tag{3.23}$$

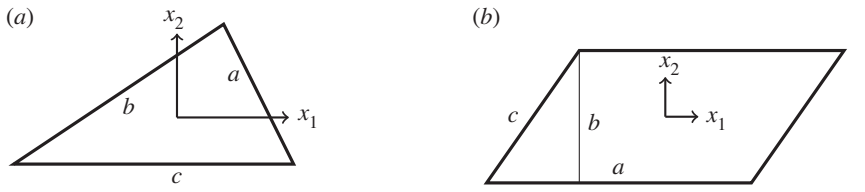

Figure 7. Inclusions in plane strain. (*a*) Triangular inclusion. (*b*) Parallelogramic inclusion.

For more general hexahedra lacking the rotational symmetry of a parallelepiped the axial moment function will not be even. However, in this particular case the axial moment function is even with respect to $\mathbf{u}$ when the order of the axial moment is odd, so unlike in the tetrahedral inclusion, odd order moments vanish, and the near field is approached faster. The ensuing multipolar moments are collected in table S3 in the electronic supplementary material. Figure 7*b* shows the hydrostatic stress field of a skewed parallelepiped across two different cross-sections: on the top surface and on the epicentral cross-section along the $x_2 = 0$ direction. These two cross-sections permit studying the effect symmetries in the shape of the inclusion have in its long- and short-range elastic fields. The symmetry of this specific inclusion means the long-range hydrostatic field at the epicentral plane vanishes, but not enough to suggest the same should happen in the near field. As the order of multipolar expansion increases, the hydrostatic field is seen to not vanish in the near field. In a highly non-symmetrical plane, the far field remains centred at the origin, though this is only a feature of the dipolar term. Convergence in the near field on opposite faces is not as fast as the force multipoles remain centred at the origin due to the skewed parallelepiped.

(f) Multipolar moments in plane strain

In the case of plane strain conditions, the polytopes of interest degenerate into planar polygons. In plane strain, these polygons represent infinite prysms, of which only a transverse section is being studied. Regardless, the whole mathematical apparatus presented here can be readily adapted to deal with plane strain polytopes. Thus, the multipolar expansion of its elastic field (equation (2.9)) remains valid over $\mathbf{x} \in \mathbb{R}^2$, $i, j, k_1, \ldots, k_n, k \in \{1, 2\}$. The general expression of the multipolar moments themselves remain valid, only that the integral is now over $\mathbb{R}^2$, Green's function itself is now the plane strain Green's function (see e.g. eqn (5.24) in Mura [23]) and $\chi_D(\mathbf{x})$ is likewise a characteristic function in $\mathbb{R}^2$. The sole term that requires being adapted to the planar conditions is equation (3.19). This may be done presently as indicated in [41]. In particular, if $d = 2$ denotes the dimensionality of the problem, then for planar cases: (1) the multiindex becomes $I = (i_1, i_2)$; (2) the vertices $\mathbf{v}_k$ will still number N, but a simple polytope in two dimensions has only two incident edges per vertex, so the tangent cone is simplified to $\mathcal{K}_v = \{\omega_1(\mathbf{v}), \omega_2(\mathbf{v})\}$; (3) thus, the axial moment function takes the form:

$$\gamma^{(|I|)}(\mathbf{z}) = -\frac{|I|!}{(|I|+2)!} \sum_{\mathbf{v}_k \in \mathcal{V}} (\mathbf{v}_k \cdot \mathbf{z})^{|I|+2} \frac{|\det \mathcal{K}_{\mathbf{v}_k}|}{(\omega_1(\mathbf{v}_k) \cdot \mathbf{z})(\omega_2(\mathbf{v}_k) \cdot \mathbf{z})}. \tag{3.24}$$

For instance, for the triangle of sides a, b, c, origin in the centroid and the x_1 axis aligned with the side c as shown in figure 7*a*, we find that

$$\gamma^{(j)}(\mathbf{u}) = \frac{2|cs|}{u_1(u_1(a^2 - b^2 - c^2) - 2cu_2 s)(u_1(a^2 - b^2 + c^2) - 2cu_2 s)} \cdot \left[\frac{2u_1}{3^{j+2} c^j} (2cu_2 s - a^2 u_1 + b^2 u_1)^{j+2} \right.$$

$$+\frac{1}{6^{j+2}c^{j+2}}(2cu_2s-u_1(a^2-b^2+c^2))(a^2u_1-2cu_2s-b^2u_1-3c^2u_1)^{j+2}$$
$$+\frac{1}{6^{j+2}c^{j+2}}(u_1(a^2-b^2-c^2)-2cu_2s)(a^2u_1-2cu_2s-b^2u_1+3c^2u_1)^{j+2}\Bigg] \tag{3.25}$$

where $s=\sqrt{b^2-((-a^2+b^2+c^2)^2/4c^2)}$. Naturally, in this case $\gamma^{(1)}(\mathbf{u})=0$, as the origin is located in the centroid, but there is no symmetry with respect to either axis, so all other moments do not vanish, $\gamma^I(\mathbf{u})\neq 0\forall|I|>1$, which means that generally the far fields of the triangular inclusion in plane strain will decay with $1/r^2$ and the near-field progress with $1/r^3$, $1/r^4$, etc. The exception would be the highly symmetrical equilateral triangle of side (say) a, in which case

$$\gamma^{(j)}(\mathbf{u})=\frac{2a^{j+2}}{\sqrt{3}(u_1^3-3u_1u_2^2)}\left[-\frac{u_1u_2^{j+2}}{3^{\frac{j}{2}}}+\frac{1}{2^{j+3}3^{j+1}}\left(u_1+\sqrt{3}u_2\right)\left(\left(3u_1-\sqrt{3}u_2\right)\right)^{j+2}+\right.$$
$$\left.+\frac{1}{2^{j+3}3^{j+1}}\left(u_1-\sqrt{3}u_2\right)\left(-\left(3u_1+\sqrt{3}u_2\right)\right)^{j+2}\right]. \tag{3.26}$$

In this case, the axial moment function is even with respect to u_1, which means that all multipolar moments where $i_1 \bmod 2\neq 0$ will vanish. As a result, the triangular inclusion in plane strain has the rare property of its near field decaying more slowly along the x_1-direction than the x_2-direction. Similar conclusions can be drawn by considering the axial moment function of other planar polytopes. For instance, for the parallelogramic inclusion of sides a and c and height b shown in figure 7*b*, the translational symmetry entails an odd axial moment function:

$$\gamma^{(j)}(\mathbf{u})$$
$$=\frac{|ab|}{2^{j+2}au_1(bu_2+cu_1)}[a^2u_1^2(-(-au_1+bu_2+cu_1)^j+(au_1+bu_2+cu_1)^j+(-au_1-bu_2-cu_1)^j$$
$$-(au_1-bu_2-cu_1)^j)+2au_1(bu_2+cu_1)((-au_1+bu_2+cu_1)^j+(au_1+bu_2+cu_1)^j$$
$$+(-au_1-bu_2-cu_1)^j++(au_1-bu_2-cu_1)^j)+(bu_2+cu_1)^2(-(-au_1+bu_2+cu_1)^j$$
$$+(au_1+bu_2+cu_1)^j+(-au_1-bu_2-cu_1)^j--(au_1-bu_2-cu_1)^j)] \tag{3.27}$$

and accordingly $\gamma^I_{\text{parall}}=0 \quad \forall I:|I| \bmod 2\neq 0$.

(g) Symmetry, parity and decay of the elastic fields of a polytopal inclusion

A key feature of the study of the multipolar moments of polytopes is that the polytope's own symmetry (indeed, any inclusion's) is reflected in the axial moment function. This follows from the formal definition of the axial moment function of a general inclusion:

$$\gamma^{(j)}(\mathbf{u})=\int(\mathbf{u}\cdot\mathbf{x})^j\chi_P(\mathbf{x})\,\mathrm{d}\mathbf{x}.$$

If the inclusion is symmetric with respect to the direction x_k, then $\chi_P(-x_k)=\chi_P(x_k)$ (all other directions omitted), and therefore by Fubini's theorem, all even ordered axial moments, $\gamma^{(2j)}(\mathbf{u})$, are likewise an even function in the direction u_j. Thus, the symmetry of an inclusion is directly mirrored by the parity of its $\gamma^{(j)}(\mathbf{u})$ axial moments. Furthermore, as shown via equation (3.19) all non-axial multipolar moments are derivatives at the origin of $\gamma^{(j)}(\mathbf{u})$. In light of this, the property whereby the derivative of an even function is odd and the derivative of an odd function vanishes at the origin can be invoked to conclude that, in those axial directions with respect to which the inclusion is symmetric, the inclusion's even ordered multipolar moments must vanish.

Thus, symmetric polytopal inclusions have no even ordered multipolar moments. This property has already been observed for the particular case of the ellipsoidal inclusion: its even ordered multipolar moments vanished because this made the integrand in the moment integrals odd with respect to the ellipsoid's measure itself. However, because a general convex polytope of N vertices will not necessarily be symmetric in any one axial direction, it is not possible to make

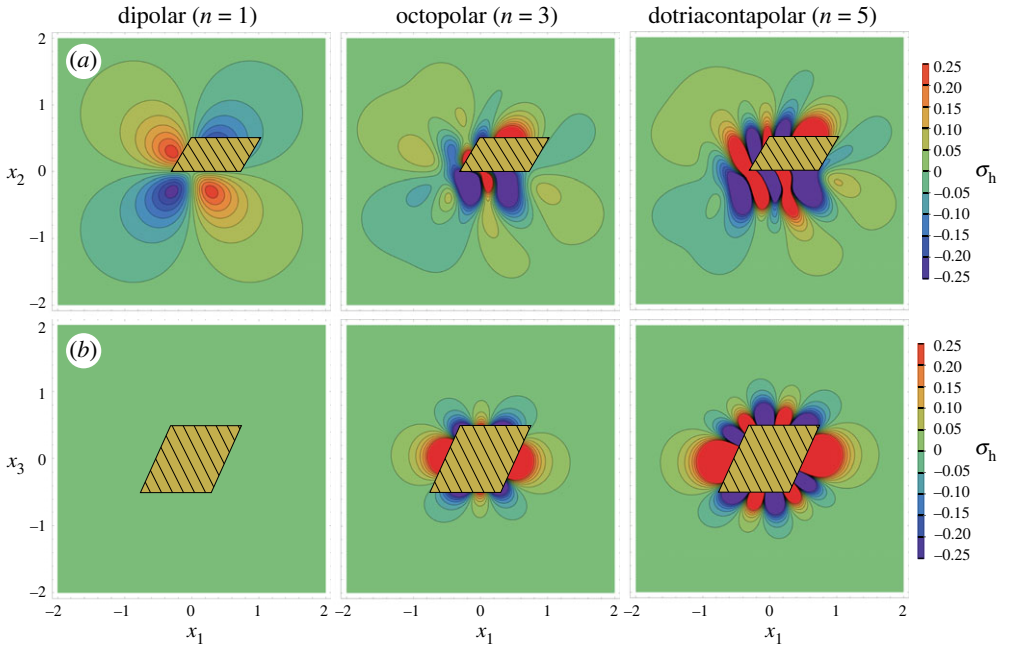

Figure 8. The hydrostatic stress field (in GPa) of a parallelepiped defined by vertices: (−1.25, −0.5, −0.5), (−0.25, −0.5, −0.5), (−0.75, 0, −0.5), (−0.25, 0, 0.5), (0.25, 0, −0.5), (1.25, 0.5, 0.5), (0.25, 0.5, 0.5), (0.75, 0, 0.5) (all units in m), with the origin placed at the centroid of the parallelepiped. The inclusion is defined as zone of constant given by the eigenstrain $e^*_{12} = 1$ (all other eigenstrain components zero). The figure depicts the cross-section on: (*a*) the upper face of the parallelepiped ($x_3 = 0.5$m); (*b*) the epicentral plane ($x_2 = 0$ m). Here $\mu = 1$ GPa, $\nu = 0.33$.

a similar general statement about the decay rate of the elastic fields of a polytopal inclusion. It is always possible to reorient the axes so as to diagonalize the multipolar moment of a given order, but this does not result in a net change in the decay rate of the fields: the multipolar moment will generally not vanish, and as was seen in the case of the hydrostatic dipolar field of the parallelepipedal inclusion considered in figure 8*b*, finding one such direction does not entail the higher odd ordered moments will vanish either.

However, when a specific polytope is symmetric with respect to one or more of the axial directions, then the same property observed in the ellipsoidal case holds: a symmetric polytope will see all its even ordered moments vanish because the integrand of the moment integral is odd with respect to the measure of $\mathbb{R}^3$. As a result, the second-order terms in the expansion will vanish and the far field of the polytope's stress field will decay with $1/r^3$, whereas the near field with $1/r^5$. Thus, whenever symmetry is present, the formulation derived here will express said symmetry through the parity of the polytope's axial moment function $\gamma^{(j)}(\mathbf{u})$: $\gamma^{(j)}(\mathbf{u})$ will be even with respect to the direction u_k, and it will follow that all even ordered multipolar moments will vanish, resulting in a net decay rate of its elastic fields that propagates in even powers of $1/r^2$. For instance, when considering the regular dodecahedron of side c, its axial moment (shown in the electronic supplementary material) function is even, meaning that $\gamma^{(j)}_{\mathrm{dod}}(-\mathbf{u}) = \gamma^{(j)}_{\mathrm{dod}}(\mathbf{u})$. Accordingly, relative to the basis it is expressed in, the dodecahedral inclusion will see all its even ordered moments vanish, i.e.

$$\gamma^I_{dod} = 0 \quad \forall I \in \mathbb{N}^3 / \, |I| \bmod 2 \neq 0. \tag{3.28}$$

Likewise conclusions are drawn for the parallelepipedal inclusion, as its axial moment function (equation (3.23)) reflects its symmetry.

Because this property is entirely dependent on the symmetry of the polytope itself, it seems clear that in practice such fast decay of the elastic fields of the polytopal inclusion will be limited to a very narrow number of cases, and that in practice most polytopal inclusions found in real materials will have a full multipolar expansion. This result is highlighted because, given that symmetry plays such a strong role in the speed with which its elastic fields decays, any attempt at modelling inclusions that relies on polytopal inclusions of high symmetry is bound to misrepresent the fields of polytopal inclusions of the same graph, unless attempts are made by the modeller at perturbing the symmetry of the base model itself: one should not approximate an irregular cuboid with a regular one, nor a faceted thin martensitic needle with an ellipsoid, for in both cases the asymmetry radically alters all near-field interactions.

4. Conclusion

This article has derived the elastic multipolar field expansions of ellipsoidal and polytopal inclusions, including a general formula for calculating all multipolar moment of ellipsoidal inclusions, and using recent developments in integer point enumeration theory, the multipolar moments of arbitrary polytopal inclusions. The approach has enabled us to show that the symmetry of the polytope is reflected by the axial moment function, and that the multipolar moments can be generated through this function. This result has been applied to specific polytopes (triangles, parallelograms, tetrahedrons, parallelepipeds and dodecahedrons), and can be used to represent any polytopal inclusion through triangulation.

We have shown that the first order dipolar terms in the expansion verify the Eshelby property that the long-range behaviour of an inclusion depends solely on its volume, regardless of its shape. Our formulation provides a bound to this far field, as well as being able to model the near-field: at a distance of about the representative size of the inclusion, the far-field dominates. Whereas the far-field is shape-insensitive, our approach has enabled us to highlight the role symmetry plays in the near field by virtue of the symmetry/parity property of the axial moment function. We have shown how symmetrical inclusions such as ellipsoids have a near-field with a $1/r^5$ decay rate, whereas non-symmetrical inclusions such as tetrahedrons have a stronger $1/r^4$ decay rate. This suggests that simplified symmetrical models will underestimate near-field interactions, and emphasizes the need for accurate geometric modelling; e.g. when twins are assimilated to ellipsoids, their near field interactions will be under-predicted.

The formulation derived here enables very accurate and very simple estimates of the elastic fields of the polytopal and ellipsoidal inclusions to arbitrary levels of accuracy for a fraction of the computational cost associated with evaluating their exact fields analytically or, more typically, through numerical approaches. As such, they will be useful in any application where knowledge of the elastic field of an inclusion is required to quantify other physical quantities. This is the case for instance when estimating diffusional flows around complex inclusions: the multipolar fields derived here enable quick and accurate estimates of the far- and near- hydrostatic stress field, which when coupled to the diffusional problem facilitates analytical estimates of the diffusional flows, as may be necessary in e.g. studying vacancy segregation around inclusions or hydrogen transport around precipitates. Likewise, the multipolar fields offer a quick method to compute with accuracy the elastic interactions between inclusions and other defects such as for instance dislocations, shear bands, or cracks; this will facilitate the modelling of such effects as precipitation hardening or the effect of impurities in discrete dislocation models of crystal plasticity, or to model faceted twins or martensitic phases and study their mutual interactions or their interactions with other defects. Further, the multipolar fields derived here enable simple estimates not only of the elastic fields, but also of the elastic energy densities of polytopes, which can be used to estimate inclusion morphologies when coupled with interfacial energy. Finally, the multipolar stress fields will also be useful in homogenization approaches reliant on computing the collective elastic fields of ensembles of inclusions, as the latter can reliably be approximated via multipolar fields presented here.

Data accessibility. In the supplementary material, an appendix containing proofs and tables of multipolar moments for different polytopes is included, and Mathematica notebook is provided to enable the computation of the multipolar fields of inclusions with any desired combination of elastic constants and dimensions data [59].

Declaration of AI use. We have not used AI-assisted technologies in creating this article.

Authors' contributions. B.G.: conceptualization, formal analysis, funding acquisition, investigation, methodology, project administration, software, validation, visualization, writing—original draft, writing—review and editing.

Conflict of interest declaration. I declare I have no competing interests.

Funding. This work was supported by the Engineering and Physical Sciences Research Council (grant no. EP/W01579X/1).

References

1. Ramsay JG. 1980 Shear zone geometry: a review. *J. Struct. Geol.* **2**, 83–99. (doi:10.1016/0191-8141(80)90038-3)
2. Philpotts AR, Ague JJ. 2022 *Principles of igneous and metamorphic petrology*. Cambridge, UK: Cambridge University Press.
3. Khachaturyan AG. 2008 *Theory of structural transformations in solids*. Mineola, NY: Dover.
4. Bhattacharyya A, Weng G. 1994 An energy criterion for the stress-induced martensitic transformation in a ductile system. *J. Mech. Phys. Solids* **42**, 1699–1724. (doi:10.1016/0022-5096(94)90068-X)
5. Glas F. 2001 Elastic relaxation of truncated pyramidal quantum dots and quantum wires in a half space: an analytical calculation. *J. Appl. Phys.* **90**, 3232–3241. (doi:10.1063/1.1394158)
6. Pan E. 2004 Eshelby problem of polygonal inclusions in anisotropic piezoelectric full-and half-planes. *J. Mech. Phys. Solids* **52**, 567–589. (doi:10.1016/S0022-5096(03)00120-0)
7. Eshelby JD. 1957 The determination of the elastic field of an ellipsoidal inclusion and related problems. *Proc. R. Soc. Lond. A* **252**, 561–569. (doi:10.1098/rspa.1959.0173)
8. Eshelby JD. 1959 The elastic field outside an ellipsoidal inclusion. *Proc. R. Soc. Lond. A* **252**, 561–569. (doi:10.1098/rspa.1959.0173)
9. Sass SL, Mura T, Cohen JB. 1967 Diffraction contrast from non-spherical distortions–in particular a cuboidal inclusion. *Philos. Mag.* **16**, 679–690. (doi:10.1080/14786436708222768)
10. Faivre G. 1969 Déformations de cohérence d'un précipité quadratique. *Phys. Status Solidi (b)* **35**, 249–259. (doi:10.1002/pssb.19690350124)
11. Walpole LJ. 1967 The elastic field of an inclusion in an anisotropic medium. *Proc. R. Soc. Lond. A* **300**, 270–289. (doi:10.1098/rspa.1967.0170)
12. Lee JK, Barnett DM, Aaronson HI. 1977 The elastic strain energy of coherent ellipsoidal precipitates in anisotropic crystalline solids. *Metall. Trans. A* **8**, 963–970. (doi:10.1007/BF02661580)
13. Sankaran R, Laird C. 1974 Interfacial structure of platelike precipitates. *Phil. Mag.* **29**, 179–215. (doi:10.1080/14786437408213562)
14. Zhou K, Keer LM, Wang QJ. 2011 Semi-analytic solution for multiple interacting three-dimensional inhomogeneous inclusions of arbitrary shape in an infinite space. *Int. J. Numer. Methods Eng.* **87**, 617–638. (doi:10.1002/nme.3117)
15. Wu L, Du SY. 1995 The elastic field caused by a circular cylindrical inclusion–part I. *J. Appl. Mech.* **62**, 579–584. (doi:10.1115/1.2895984)
16. Hasegawa H, Lee VG, Mura T. 1992 The stress fields caused by a circular cylindrical inclusion. *J. Appl. Mech.* **59**, 107–114. (doi:10.1115/1.2899473)
17. Lee YG, Zou WN, Ren HH. 2016 Eshelby's problem of inclusion with arbitrary shape in an isotropic elastic half-plane. *Int. J. Solids Struct.* **81**, 399–410. (doi:10.1016/j.ijsolstr.2015.12.024)
18. Golgoon A, Yavari A. 2017 On the stress field of a nonlinear elastic solid torus with a toroidal inclusion. *J. Elast.* **128**, 115–145. (doi:10.1007/s10659-016-9620-3)
19. Ru C. 1999 Analytic solution for Eshelby's problem of an inclusion of arbitrary shape in a plane or half-plane. *J. Appl. Mech.* **66**, 315–523. (doi:10.1115/1.2791051)
20. Rodin GJ. 1996 Eshelby's inclusion problem for polygons and polyhedra. *J. Mech. Phys. Solids* **44**, 1977–1995. (doi:10.1016/S0022-5096(96)00066-X)
21. Zhou K, Hoh HJ, Wang X, Keer KM, Pang JHL, Song B, Wang QJ. 2013 A review of recent works on inclusions. *Mech. Mater.* **60**, 144–158. (doi:10.1016/j.mechmat.2013.01.005)

22. Bouwkamp CJ, Casimir HBG. 1954 On multipole expansions in the theory of electromagnetic radiation. *Physica* **20**, 539–554. (doi:10.1016/S0031-8914(54)80068-1)
23. Mura T. 1982 *Micromechics of defects in solids*, 2nd edn. Amsterdam, The Netherlands: Kluwer Academic Publishers.
24. Kanzaki H. 1957 Point defects in face-centred cubic lattice–I distortion around defects. *J. Phys. Chem. Solids* **2**, 24–36. (doi:10.1016/0022-3697(57)90003-3)
25. Sinclair JE. 1979 Epicentre solutions for point multipole sources in an elastic half-space. *J. Phys. D: Appl. Phys.* **12**, 1309. (doi:10.1088/0022-3727/12/8/010)
26. Schober HR, Ingle KW. 1980 Calculation of relaxation volumes, dipole tensors and Kanzaki forces for point defects. *J. Phys. F: Met. Phys.* **10**, 575–581. (doi:10.1088/0305-4608/10/4/009)
27. Dudarev SL, Ma PW. 2018 Elastic fields, dipole tensors, and interaction between self-interstitial atom defects in bcc transition metals. *Phys. Rev. Mater.* **2**, 033602. (doi:10.1103/PhysRevMaterials.2.033602)
28. Dederichs PH. 1973 The theory of diffuse X-ray scattering and its application to the study of point defects and their clusters. *J. Phys. F: Met. Phys.* **3**, 471. (doi:10.1088/0305-4608/3/2/010)
29. Backus G, Mulcahy M. 1976 Moment tensors and other phenomenological descriptions of seismic sources—I. Continuous displacements. *Geophys. J. Int.* **46**, 341–361. (doi:10.1111/j.1365-246X.1976.tb04162.x)
30. Backus G, Mulcahy M. 1976 Moment tensors and other phenomenological descriptions of seismic sources—II. Discontinuous displacements. *Geophys. J. Int.* **47**, 301–329. (doi:10.1111/j.1365-246X.1976.tb01275.x)
31. Sarkar S, Čebron M, Brojan M, Košmrlj A. 2021 Method of image charges for describing deformation of bounded two-dimensional solids with circular inclusions. *Phys. Rev. E* **103**, 053004. (doi:10.1103/PhysRevE.103.053004)
32. Dudarev SL, Sutton AP. 2017 Elastic interactions between nano-scale defects in irradiated materials. *Acta Mater.* **125**, 425–430. (doi:10.1016/j.actamat.2016.11.060)
33. Gurrutxaga-Lerma B. 2018 Static and dynamic multipolar field expansions of dislocations and cracks in solids. *Int. J. Eng. Sci.* **128**, 165–186. (doi:10.1016/j.ijengsci.2018.03.012)
34. Gurrutxaga-Lerma B. 2019 A stochastic study of the collective effect of random distributions of dislocations. *J. Mech. Phys. Solids* **124**, 10–34. (doi:10.1016/j.jmps.2018.10.001)
35. LeSar R, Rickman JM. 2002 Multipole expansion of dislocation interactions: application to discrete dislocations. *Phys. Rev. B* **65**, 144110. (doi:10.1103/PhysRevB.65.144110)
36. Wang Z, Ghoniem N, LeSar R. 2004 Multipole representation of the elastic field of dislocation ensembles. *Phys. Rev. B* **69**, 174102. (doi:10.1103/PhysRevB.69.174102)
37. Vakulenko AA, Kosheleva AA. 1980 Some problems of the theory of elasticity of composite media. *Vestnik Leningradskogo Gosudarstvennogo Universiteta (Trans. Leningrad State University, in Russian), Ser. Math. Mech. Astron*, pp. 125–135.
38. Kosheleva AA. 1983 Method of multipolar expansion in the mechanics of matrix composites. *Mech. Compos. Mater.* **19**, 301–307. (doi:10.1007/BF00604395)
39. Kushch VI. 2013 *Micromechanics of composites: multipole expansion approach*. London, UK: Butterworth-Heinemann.
40. Eshelby JD. 1961 Elastic inclusions and inhomogeneities. In *Progress in solid mechanics* (eds IN Sneddon, R Hill), vol. II, pp. 89–140. Amsterdam, Netherlands: North-Holland.
41. Beck M, Robins S. 2007 *Computing the continuous discretely*, vol. 61. Undergraduate Texts in Mathematics. New York, NY: Springer.
42. Petrowsky I. 1945 On the diffusion of waves and the lacunas for hyperbolic equations. *Matematicheskii Sbornik* **17**, 289–370.
43. Atiyah M, Bott R, Gårding L. 1970 Lacunas for hyperbolic differential operators with constant coefficients. I. *Acta Math.* **124**, 109–189. (doi:10.1007/BF02394570)
44. Atiyah M, Bott R, Gårding L. 1973 Lacunas for hyperbolic differential operators with constant coefficients. II. *Acta Math.* **131**, 145–206. (doi:10.1007/BF02392039)
45. Markenscoff X. 1997 On the shape of the Eshelby inclusions. *J. Elast.* **49**, 163–166. (doi:10.1023/A:1007474108433)
46. Liu LP. 2008 Solutions to the Eshelby conjectures. *Proc. R. Soc. A* **464**, 573–594. (doi:10.1098/rspa.2007.0219)
47. Burridge R, Knopoff L. 1964 Body force equivalents for seismic dislocations. *Bull. Seismol. Soc. Am.* **54**, 1875–1888. (doi:10.1785/BSSA05406A1875)
48. Jin X, Lyu D, Zhang X, Zhou Q, Wang Q, Keer LM. 2016 Explicit analytical solutions for a complete set of the Eshelby tensors of an ellipsoidal inclusion. *J. Appl. Mech.* **83**, 121010. (doi:10.1115/1.4034705)

49. Park JH. 2007 Formation mechanism of spinel-type inclusions in high-alloyed stainless steel melts. *Metallurgical Mater. Trans. B* **38**, 657–663. (doi:10.1007/s11663-007-9066-x)
50. Mura T. 1997 The determination of the elastic field of a polygonal star shaped inclusion. *Mech. Res. Commun.* **24**, 473–482. (doi:10.1016/S0093-6413(97)00052-9)
51. Nozaki H, Taya M. 2001 Elastic fields in a polyhedral inclusion with uniform eigenstrains and related problems. *J. Appl. Mech.* **68**, 441–452. (doi:10.1115/1.1362670)
52. Nenashev AV, Dvurechenskii AV. 2010 Strain distribution in quantum dot of arbitrary polyhedral shape: analytical solution. *J. Appl. Phys.* **107**, 064322. (doi:10.1063/1.3357302)
53. Bloomenthal J. 1988 Polygonization of implicit surfaces. *Comput. Aided Geometr. Des.* **5**, 341–355. (doi:10.1016/0167-8396(88)90013-1)
54. Brion M. 1988 Points entiers dans les polyèdres convexes. *Ann. Sci. Ecole Norm. Sup.* **21**, 653–663.
55. Barvinok AI. 1992 Exponential sums and integrals over convex polytopes. *Funct. Anal. Appl.* **26**, 127–129. (doi:10.1007/BF01075276)
56. Brion M, Vergne M. 1997 Residue formulae, vector partition functions and lattice points in rational polytopes. *J. Am. Math. Soc.* **10**, 797–833. (doi:10.1090/S0894-0347-97-00242-7)
57. De Loera JA, Dutra B, Koeppe M, Moreinis S, Pinto G, Wu J. 2012 Software for exact integration of polynomials over polyhedra. *ACM Commun. Comput. Algebra* **45**, 169–172. (doi:10.1145/2110170.2110175)
58. Gravin N, Pasechnik DV, Shapiro B, Shapiro M. 2018 On moments of a polytope. *Anal. Math. Phys.* **8**, 255–287. (doi:10.1007/s13324-018-0226-8)
59. Gurrutxaga-Lerma B. 2023 The multipolar elastic fields of ellipsoidal and polytopal plastic inclusions. Figshare. (doi:10.6084/m9.figshare.c.6794100)